Arch. Metall. Mater. **67** (2022), 4, 1443-1453

DOI: https://doi.org/10.24425/amm.2022.141072

CEREN EFE[1*], YAVUZ SUN[2], YUNUS TÜREN[2], HAYRETTIN AHLATCI[2]

MICROSTRUCTURE AND TRIBOLOGICAL BEHAVIOR OF Cu-2.5Ti ALLOY IN TWO DIFFERENT ENVIRONMENTS

In this study, the nominal composition of Cu-2.5Ti alloy was thermally treated to obtain homogenized, aged, and 40% prior cold-rolled+ aged samples. The hardness, wear behavior, and microstructure of samples were investigated. The reciprocating wear tests were performed under four different loads under dry and 3.5%NaCl corrosive environments. The alloy reached its highest hardness value of 8 hours for the aged sample. The hardness value of the sample that was homogenized then cold-rolled by 40% and aged was found higher than the other samples. A decrease in the wear rates in dry conditions was observed in homogenized, aged and cold-rolled and aged samples, respectively. This decrease was more in the corrosive environment. Studies can be advanced by examining the wear behavior at different alloy ratios. The effects of different alloying elements and the ratio of cold-rolled before or after aging can also be investigated for future research.

Keywords: Cu-Ti alloys; Wear behavior; Corrosive environment; Hardness

1. Introduction

It has been found that age-hardened alloys have wide application in a variety of fields some engineering materials because of their high elastic and electrical conductivity properties. Copper-Beryllium (Cu-Be) alloys have unique mechanical properties but also the fact that the beryllium oxide gas released during the production of this material is very toxic. For this result, its production is linked to great ecological danger. Dilute Cu-Ti alloys (containing approximately 1%-5% (mass fraction) Ti) are widely known since the 1930s as a substitute for expensive and toxic Cu-Be alloys [1]. They can be applied for the production of high-strength springs as well as elements resistant to corrosion and abrasion, as electronic components, electrical connections, contacts, relays, electrical wires, gears, and as components of equipment for anti-terrorist and mining rescue units compared to those of Cu-Be [2]. The equilibrium phase in the Cu-Ti system is usually formed by classical Widmanstatten or cellular precipitation. The cellular or 'discontinuous' precipitation reaction plays a central role in the extreme aging of these high-strength alloys [1]. Since the mechanical properties of Cu-Ti alloys are critically affected by their precipitation behavior, it is important to understand the volume fraction and composition changes that accompany the morphological and structural evolution of α-Cu4Ti and β-Cu4Ti precipitates during aging [3]. Numerous studies [4-7] have shown that the metastable β'-Cu4Ti phase formed during aging enhances the strengthening effect; however, if the sufficient aging temperature or aging time is exceeded, the phase transformation from the metastable and compatible β'-Cu4Ti phase to the equilibrium and incoherent Cu3Ti phase occurs, and thus the strength of the Cu-Ti alloys is significantly reduced. There are some of the studies in the literature have centered of attention such as on the formability of Cu-Ti alloys with various Ti content and the effects of deformation conditions, thermal processes with mechanical properties and electrical properties [2,8] and some of them are about the effects of prior cold deformation on hardness, tensile properties, and microstructure of aged Cu-Ti alloys [3,9-11]. In a study examining the wear behavior of Cu-Ti alloys containing different amounts of Ti using the powder metallurgy method other than the casting method, an intense material transfer from the sample trace surface was observed in the wear behavior of pure Cu without Ti, and it was concluded that this situation exhibits plastic deformation due to the low hardness of pure copper. On the other hand, it was concluded that in the samples containing 3% and 5% Ti, a linear increase was observed in the hardness

[1] ZONGULDAK BÜLENT ECEVIT UNIVERSITY, GÖKÇEBEY M. M. ÇANAKCI VOCATIONAL SCHOOL OF HIGHER EDUCATION, GÖKÇEBEY, ZONGULDAK, TURKEY
[2] KARABUK UNIVERSITY, DEPARTMENT OF METALLURGY AND MATERIALS ENGINEERING, KARABUK, TURKEY

* Corresponding author: ceren.efe@beun.edu.tr

values with the increase in the Ti ratio, and accordingly, the wear resistance increased. It is useful to understand better the friction and wear performance of the Cu-Ti alloys to be able to expand their applications [12]. In the studies of the tribological behavior of Cu-3Ti and Cu-4.5Ti alloys produced by the cold forging method (multiaxial cyroforging-MAF), it was found that as the MAF cycles increased, the friction coefficient decreased due to the increase in hardness. They found that as the load increases, the COF value also increases [13,14].

This study's difference is the role of microstructure with a different degree of strengthening of the Cu- 2.5wt.%Ti alloy and its influence on the values of the friction coefficient and the degree of wear in tribological tests. In this present work, reciprocating wear tests were applied Cu-2.5Ti alloy after homogenized, peak aged and prior cold-rolled and aged under two different environment dry and 3.5% NaCl water solution conditions at room temperature. The effects of normal load on its friction coefficient and wear performance were investigated. The wear surfaces were studied, to get a better understanding of the wear mechanism and wear behavior of the alloy under a dry and corrosive environment.

2. Experimental

Cu-2.5Ti alloy with traces of aluminum and rare earth was produced in a vacuum induction furnace. The chemical composition of alloy was measured with a wavelength dispersive X-ray fluorescence spectrometer (Rigaku Primus II) and is given in TABLE 1. As raw materials, pure electrolytic copper and titanium metal were melted as an ingot with a nominal composition of Cu- 2.5%Ti by induction vacuum under argon atmosphere. Plates with a thickness of 20 mm are cut from the ingot. A part of the plate was heat-treated at 900ºC for 24 h. for homogenization(H), solution treated (ST) at 850°C for 2 h. followed by water quenching and aged at 450°C for 8 h (AG). The other part of the plates was also heat-treated under the same condition and then cold-rolled by 40% at room temperature followed by aging 450°C for 8 h (CR+ AG).

TABLE 1

The chemical composition of Cu-2.5%Ti alloy

Elements, wt %	Al	P	S	Ti	Cu
Cu-2.5Ti	0.16	0.05	0.02	2.61	97.16

The dependence of the specimen hardness on the depth from the surface was estimated using a Vickers hardness tester (Qness, Q10 A+). The tests were carried out on a 500 g load for 10 seconds. 10 measurements were made from all samples and the average was taken.

The wear tests were carried out using a reciprocating wear tester, tribometer test device (UTS, T10/20) under normal loads of 5, 10, 20, and 40N at room temperature. Before the wear test, all the specimen surfaces were ground with 1200 grit SiC paper, cleaned with alcohol, and dried. The surface area of specimens was loaded and slid against an abrasive AISI 52100 steel ball with a hardness of 62 HRC at a sliding speed of 150 mm/s. All wear tests were performed under different environments dry and corrosive 3.5%NaCl water solution. For each environment, three tests were performed, and the average value was used for the wear graphs. The loss of wear volume was performed using the calculation in Eq. (1). were situated wear depth, wear width, and stroke distance parameters where V_w is the wear volume loss, c is the stroke distance and a, b are the wear width and depth, respectively as shown in Fig. 1 illustration. The wear width was measured with a Mitutoyo SJ-410 instrument by using a 2 mm diameter standard probe from three different places depending on the depth (b) and width (a) of the wear trace. The worn surfaces of the specimens were examined using scanning electron microscopy (SEM) and energy-dispersive X-ray spectroscopy (EDX) for understanding the wear mechanisms.

$$V_w(\mathrm{mm}^3) = \frac{2ab}{3}c \tag{1}$$

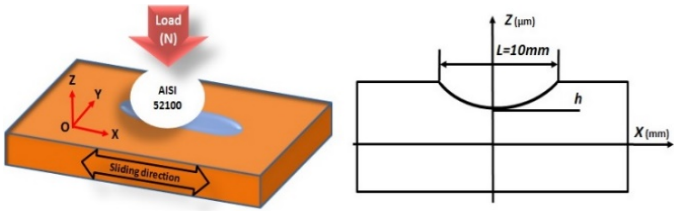

Fig. 1. Illustration of wear trace

3. Results and discussions

3.1. Hardness measurements and microstructure characterization

TABLE 2 shows the effect of aging time on the Vickers hardness of the Cu-2.5Ti alloy. In our study as cast Cu-2.5Ti alloy has 124 HV5 hardness value. The hardness value of the homogenized sample was found at 171 HV5. Solution treated process resulted in hardness reduction of the alloy from 171 HV5 to 85 HV5 after homogenization. In the study of Szkliniarz for the Cu-3Ti alloy, this value resulted in a decrease from 163 HV10 to 103 HV10 with the solution treated after homogenization [8]. The solution treatment of titanium bronzes usually takes place at about 900°C. Thus, small Cu and Ti intermetallic precipitates remain in the microstructure after the homogenization process is dissolved [1,8,12-16]. For the applications in engineering and investigating fundamental aspects of hardening phenomena in Cu-Ti alloy system, the decomposition during aging between 300º and 500ºC is understood well including spinodal decomposition, with compositional fluctuations, formation of a coherent, metastable phase called β' and equilibrium phase β by a discontinuous or cellular reaction [14-16]. In Fig. 2a there are seen polygonal particles in the homogenized sample. At the temperature of 450ºC, grain boundaries and heterogeneously precipitated par-

TABLE 2

Variation of Vickers hardness of the Cu-2.5wt.% Ti alloy with aging time and different heat treatments

Cu-2.5Ti	Vickers Hardness (HV5)				
As cast	124				
(H)	171				
(ST)	85				
	Aging time				
(AG)	2 hours	4 hours	8 hours	16 hours	24 hours
	206	220	**235**	236	169
(CR+AG)	**272**				

ticles were observed in the aged (AG) sample (Fig. 2b and also in Fig. 5). The alloy reached its highest hardness value of 235 HV5 in 8 hours (AG). As seen from TABLE 2 prolonged aging times cause a decrease in hardness values. This is because of the characteristic effects of discontinuous precipitation at the grain boundaries of the aged alloy, which can be seen especially after long aging times [1,8,9,11,17]. The hardness value of the sample that was homogenized then cold-rolled by 40% at room temperature followed by solution treated and aged (CR+ AG) was found 272 HV5. In the study of Nagarjuna et. al. aging of cold-worked Cu-1.5Ti and Cu-4.5Ti alloys result in the formation of fine, ordered, metastable and coherent Cu_4Ti, continuous β precipitates having body-centered tetragonal (BCT) crystal structure [10], which is also reported to be the strengthening phase in Cu-Ti alloys [11,18]. It can be said that striated precipitates occur in a 40% cold deformed state of the sample as seen in Fig. 2c attributed to the deterioration of equiaxed grains due to cold deformation. In the EDX analysis observed intersecting crystallographic planes were observed in a rather flat form. A similar structural form was also reported in the study of Nagarjuna et al. [19]. Hardness critically depends on the ease with which dislocations move. Strengthening of deformed and aged alloys resulting from the formation of titanium-rich coherent precipitates is accelerated by enhanced diffusion, due to an increase of vacancy concentration introduced by deformation [17]. Similar behavior was reported by increasing the amount of cold work (0-80%) caused an increase in the peak hardness in the study of Nagarjuna et. al. [9].

SEM micrograph and EDX analysis results of Cu-2.5Ti alloy of H sample are given respectively in Fig. 3 and Fig. 4 The alloy appears to contain a single supersaturated Cu solid solution

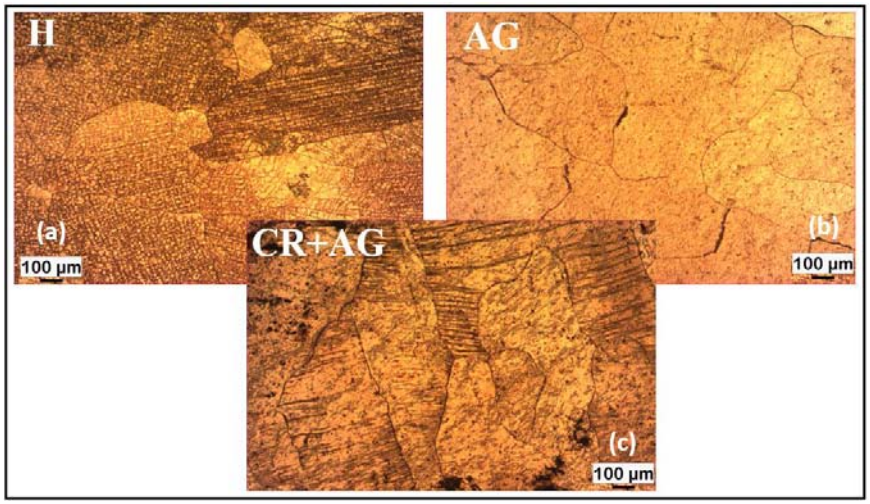

Fig. 2. Optical micrographs from the surfaces of the etched Cu-2.5Ti alloy. Mag = 50× (a) sample (H), (b) sample (AG), (c) sample (CR+ AG)

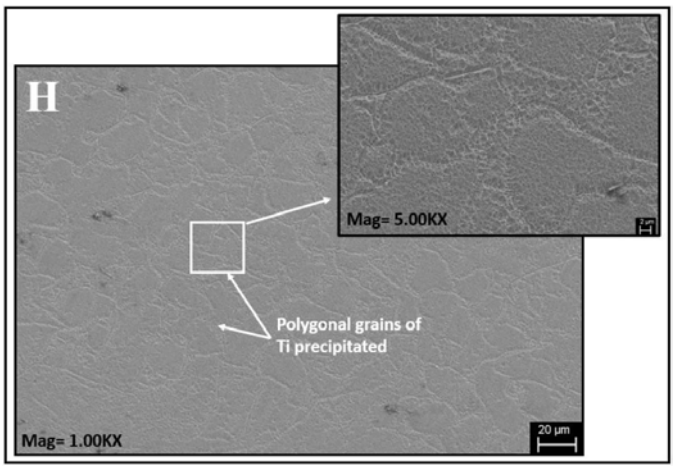

Fig. 3. SEM micrograph of homogenized Cu-2.5Ti sample

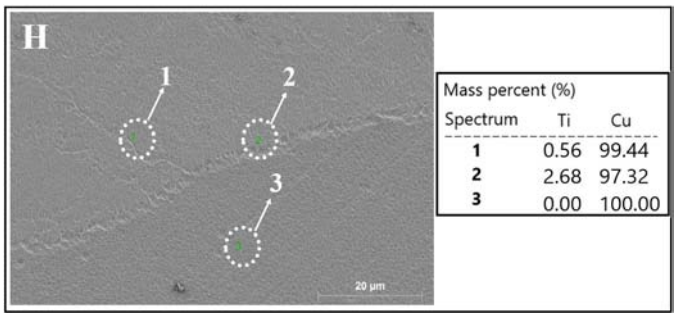

Fig. 4. EDX analysis of homogenized Cu-2.5Ti sample

phase (as seen in XRD results from Fig. 9) with recrystallization grains (polygonal grains). Ti-rich small precipitates can be seen at grain boundaries. In the SEM micrograph of the aged

sample (AG) in Fig. 5, fine needle-shaped precipitates dispersed throughout the grain, and a small number of cellular precipitates advancing from the grain boundaries into the grains are seen together. From EDX analysis in Fig. 6. it can be said that abundant fine precipitates consisting of coherent, metastable, and continuous β-Cu_3Ti phase with a body-centered tetragonal structure are observed in the AG sample. In addition, the grain boundaries in the AG sample appear much sharper and finer compared to the H sample. It has been reported that the volume fraction of these cellular precipitates (compared to needle-shaped precipitates) increases with increasing aging time (prolonged aging), and cellular precipitates become dominant in the sample [3,19,20].

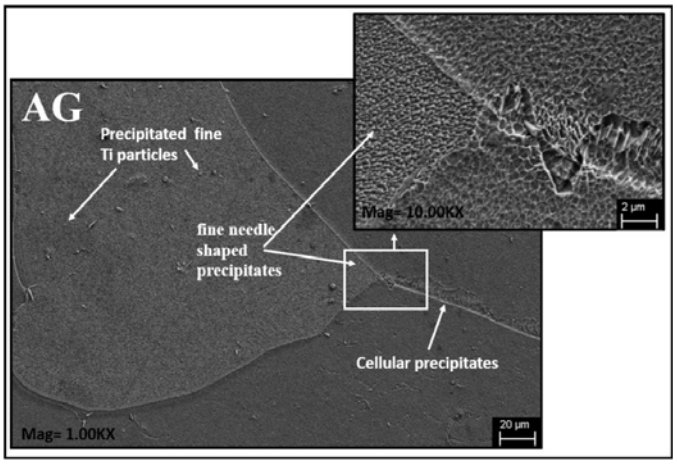

Fig. 5. SEM mocrograph of aged Cu-2.5Ti sample

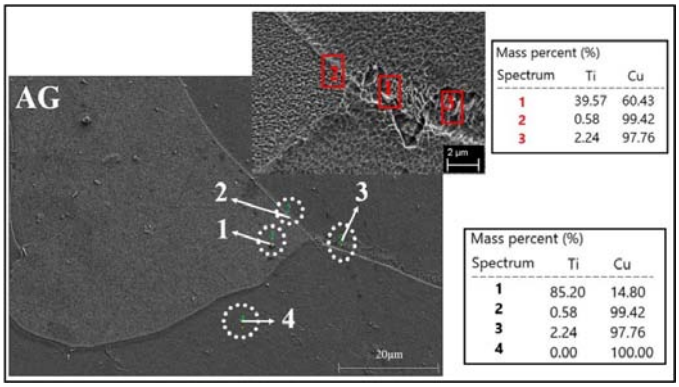

Fig. 6. EDX analysis of aged Cu-2.5Ti sample

SEM mocrograph and EDX analysis results of CR+ AG sample of Cu-2.5Ti alloy are given in Fig. 7 and Fig. 8, respectively. Compared to the H and AG samples, it was observed that metastable β-Cu_3Ti continuous particles were widely distributed, although no clear grain boundaries were observed in the CR+ AG sample. Band-like formations are observed in the sample with 40% deformation. It has been reported in Nagarjuna's study that these bands occur due to twinning, and with the increase in the amount of deformation, the distance between the bands decreases to almost nothing and approaches each other [19].

From Fig. 9 XRD profiles generally showed peaks from the Cu solid solution and β-Cu_3Ti phases, but no peaks from the

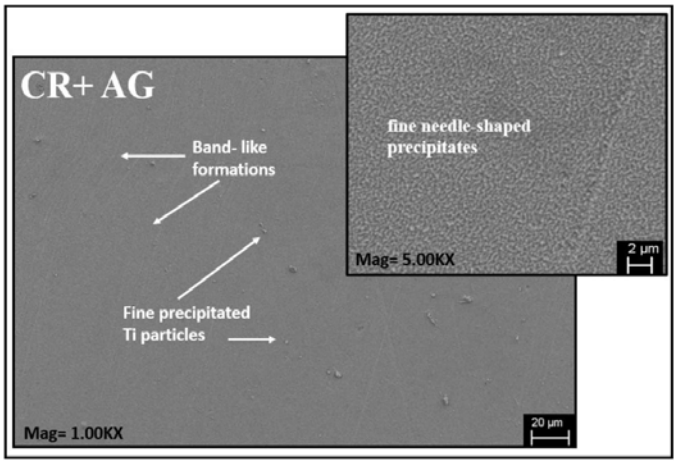

Fig. 7. SEM micrograph of 40% cold-rolled and aged Cu-2.5Ti sample

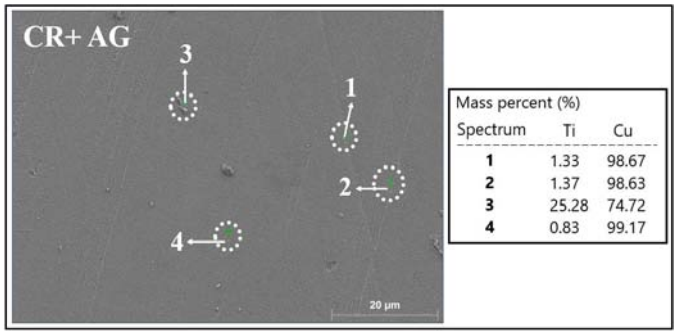

Fig. 8. EDX analysis of 40% cold-rolled and aged Cu-2.5Ti sample

α-Cu_3Ti phase. Water solution treatment of the previously homogenized alloy at 850°C causes almost complete dissolution of the intermetallic Cu_3Ti phase precipitates. In the microstructure of the CR+ AG sample, the intermetallic Cu_3Ti phase form of characteristic lamellar precipitates can not be seen obviously as in the aged one (see Fig. 5 and Fig. 7). This situation is described in A. Szkliniarz's study as the precipitates of the intermetallic Cu_3Ti phase undissolved under the solution treatment conditions that occur at the uniaxial grain boundaries are visible only

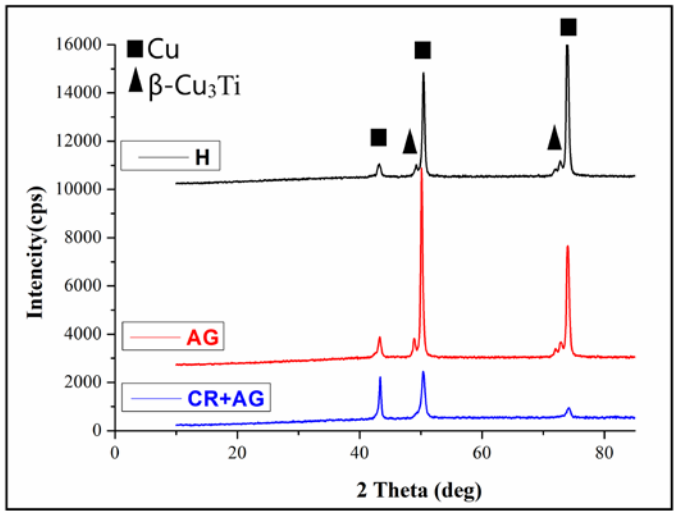

Fig. 9. XRD patterns of Cu-2.5Ti samples

after the solution treatment. After aging in a short time like one hour to four hours the alloy reaches its maximum hardness does not result in significant changes in its microstructure. Major microstructural changes in the form of the characteristic lamellar precipitates occurring at the grain boundaries as a result of discontinuous precipitation are visible only after the alloy that has been overaged (48 h) [8].

3.2. Wear behavior of Cu-2.5Ti alloy

Load dependence and wear tests:

From the examination of the variation of the friction coefficients (COF) with the sliding distance of 1000 m and sliding speed of 150 mm/s under dry conditions and various normal loads for the Cu-2.5Ti alloy, it was found that during the initial sliding distance, the frictional coefficient had remained unstable for both samples and then maintained nearly steady state (after ~100 m) until the termination of the tests as seen in Fig. 10 for the applied 10 N normal load. The same situation is seen in the figure also showed a similar trend in the other load applications. With the increasing sliding distance, fluctuation of friction coefficients indicates that there was some metallic transfer between the sliding materials, as it happens by the nature of under dry sliding conditions. During steady-state, a friction layer forms, removing wear debris from the sliding pair. As a result of the wear process, a hardened surface layer is produced in copper and its alloys, as described in a previous literature study [20]. From Fig. 11 it can be said the friction coefficient of specimens depends on the environment. It is seen that in a corrosive 3.5%NaCl water solution environment the friction coefficients are lower than the dry one. It can be thought that the corrosive environment affected the contact of the two layers at the sliding interface to reduce friction and wear and to remove the heat generated during friction. It seems that liquid change controlling steps of wear and performs like a lubricant. The reason for the peaks in Fig. 11 can be shown as corrosion products created in more aggressive conditions decrease friction coefficients of all samples. In general, friction and wear at the contact surfaces depend significantly on the relationship between the physical state of the contacting interfaces and the chemical interactions between the sliding interfaces and the environment [21]. The most important factors affecting the coefficient of friction are the applied force, surface quality, and the internal structures of the materials [22].

From Fig. 12 as compared wear rates of the sample (H) with the samples (AG) and (CR+ AG) under the load of 5 N and 40 N under dry environment, the decrease in wear rates was found 24%, 75% for the applied load 5 N, and 45%, 76% for the applied load 40 N respectively. When a similar comparison is taken for corrosive environment the wear rates of the sample(H) under the load of 5 N and 40 N the decrease in wear rates of (AG) and (CR+ AG) were found 56%, 58% for the applied load 5 N and 60%, 68% for the applied load 40 N respectively. It has been observed that when the applied load is increased to 40 N a high rate of wear occurs. The decrease in wear rates of the samples (H), (AG), and (CR+ AG) can be attributed to the increase in hardness values. Higher hardness values of (AG) and (CR+ AG) of Cu-2.5Ti samples exhibit that they are mechanically more resistant and abrasion resistance. Sample with the

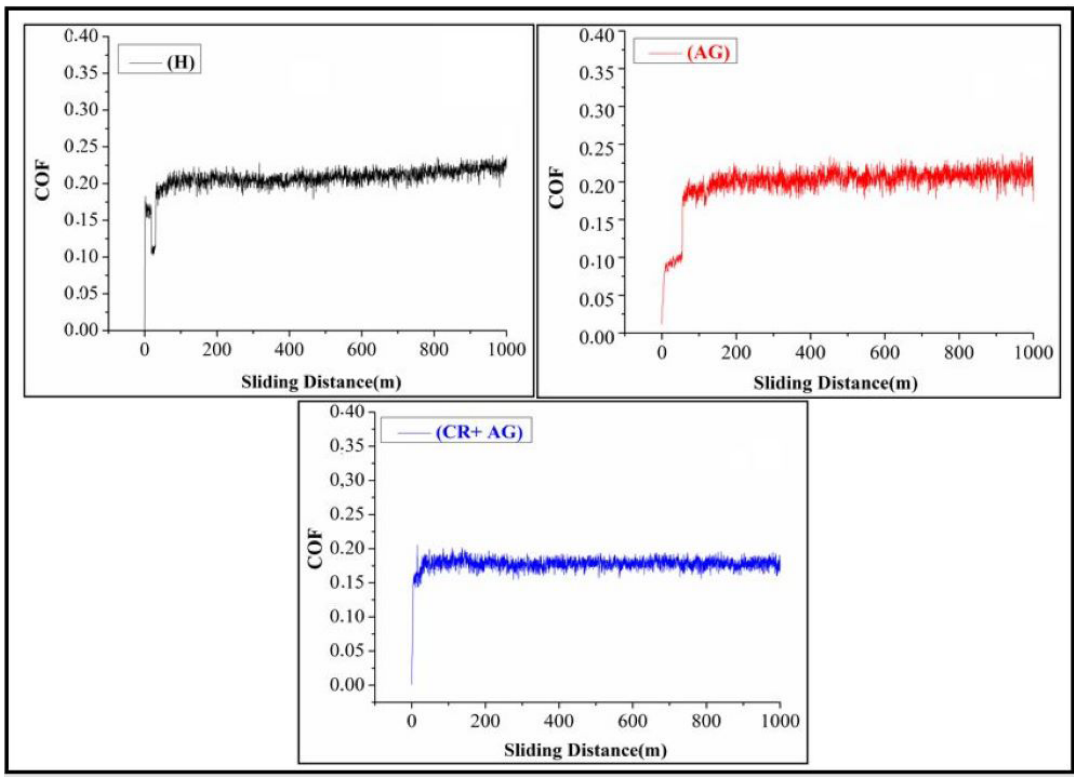

Fig. 10. Plot of variation in COF of Cu-2.5Ti with increasing sliding distance at an applied load of 10 N under dry environment

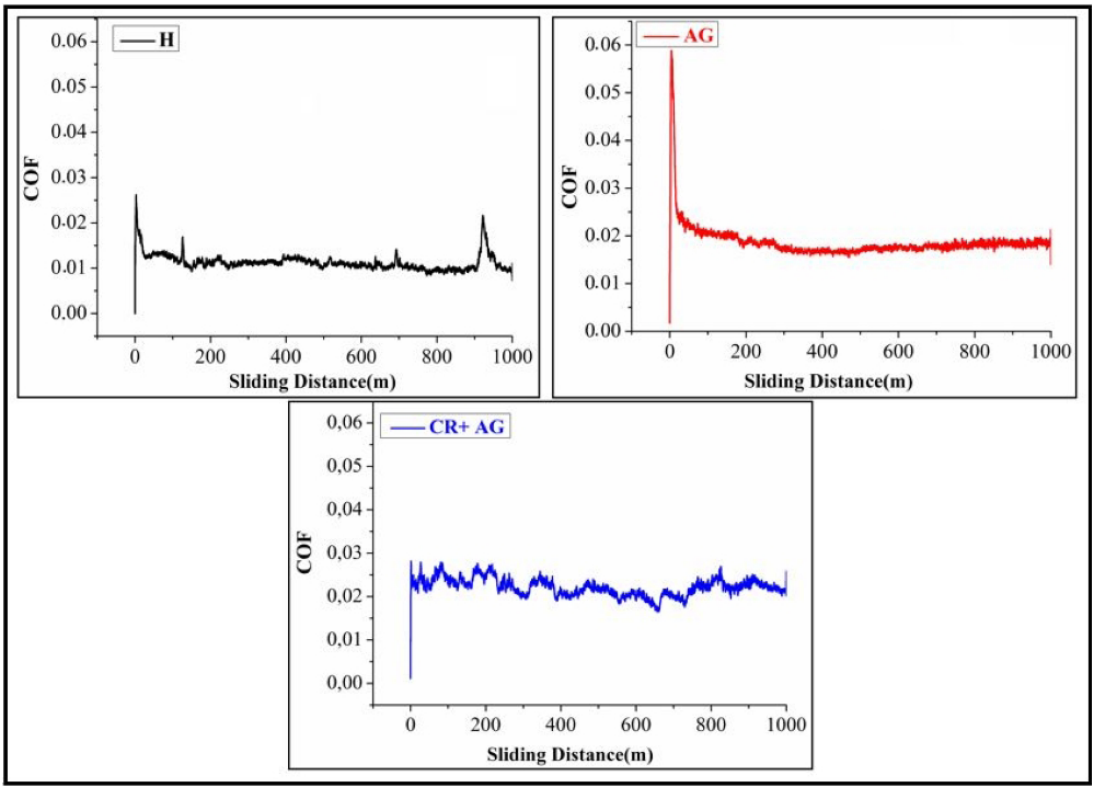

Fig. 11. Plot of variation in COF of Cu- 2.5Ti with increasing sliding distance at an applied load of 10 N under corrosive environment

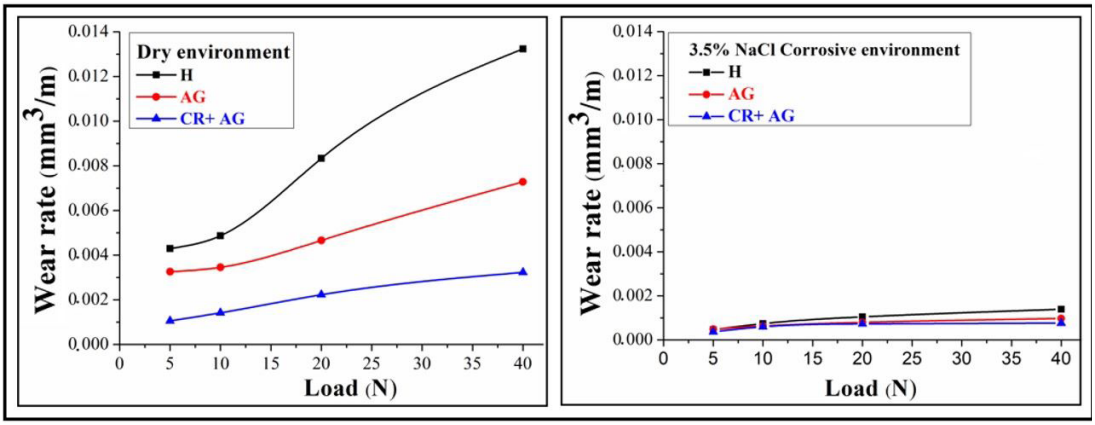

Fig. 12. Wear rates of the Cu-2.5Ti samples versus applied loads at a sliding speed of 150 mm/s. under two different environments

highest hardness (CR+ AG) showed the lowest wear rates as stated in Archard's Rule a material with high hardness exhibits lower wear rates [23].

Microscopic study of the worn surfaces:

In Fig. 13 representative SEM micrographs are showing the worn surfaces to understand the effects of the lowest and the highest applied loads of 5 N and 40 N of the samples at room temperature under a dry environment. Worn surfaces show plastic deformation regions, grooves, and debris. It can be said that the wear surfaces of the samples under 5 N load have a relatively smooth morphology. When the load amount is 40 N, it is seen that the samples produce wear residue and adhesive wear predominates in all samples. When the applied load is 40 N the edges of large flaky type debris of the H sample were folded onto itself due to its quite soft nature because of its hardness value. The removed material was smeared to the worn surface during the sliding and created a smoother surface under the applied load 40 N. For the samples AG and CR+ AG, it can be said that material delamination decreased due to the increase in hardness, which is evidence of the formation of the adhesive mechanism in these samples. Delamination produced wear debris from sub-surface cracks as a result of plow removal materials. This indicates that abrasive wear and also plastic deformation regions occur due to the increased load. According to EDX analyses in Fig. 14, the mass percentage of oxygen indicates the formation of an oxide layer on the worn surfaces on all of the samples and thus supports oxidative wear mechanisms. The oxide layer formation occurred

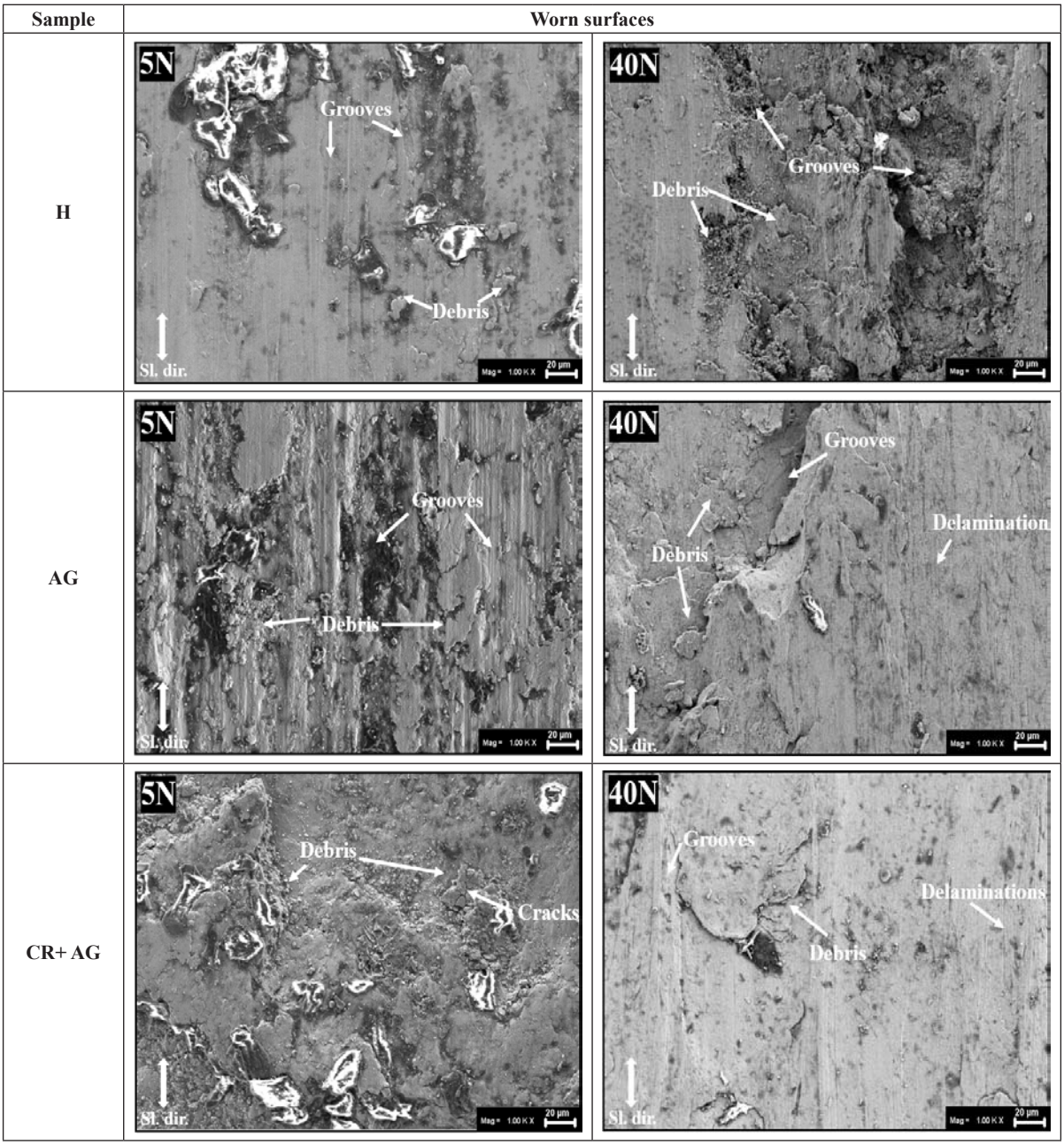

Fig. 13. SEM micrographs showing the worn surfaces of the Cu-2.5Ti alloy samples under a dry environment

on the worn surfaces which means that bright surface and brittle appearances are the results of the high oxide formations on this debris. During the sliding oxide film is tending to fracture and some cracks appear on the oxide layer. The cracked oxide layer pulls out and separates from the worn surface and forms oxide particles. These oxide particles at the later stage of the sliding generate spherical wear particles. In the EDX analysis results, it is also seen that the C peak is observed at a high rate. C and O peaks indicate transfer-back transfer between mating surfaces and oxidation as a result of frictional heat. The reason for this is also thought to be caused by dust particles that break off from the ball and stick to the surface again as a result of the interaction between the ball and the wear surface during the wear mechanism. Another reason for this can be thought also as contamination on the samples like grease, sweat.. etc. These were also expressed in many studies that the broken parts adhered to the surfaces and caused adhesive wear mechanism [24,25]. It can be said that the presence of these elements is the reason that the COF of CR+AG samples is higher than that of other alloys. The white debris on the surface looking at Fig. 13 and Fig. 15, appears to diminish and peelings correlated with adhesive wear occur in some regions of the worn surface.

The tribological tests of Cu-2.5Ti alloy were carried out also under the corrosive environment of 3.5% NaCl water solution for all samples. The SEM photographs of the worn surfaces at applied load 5 N and 40 N were shown in Fig. 15 At the applied load 5 N some tears have occurred. The surface morphology is relatively smooth for 5 N and when the load is 40 N, it seems that this surface smoothness deteriorates due to the increasing amount of load. Under the corrosive environment, the chloride

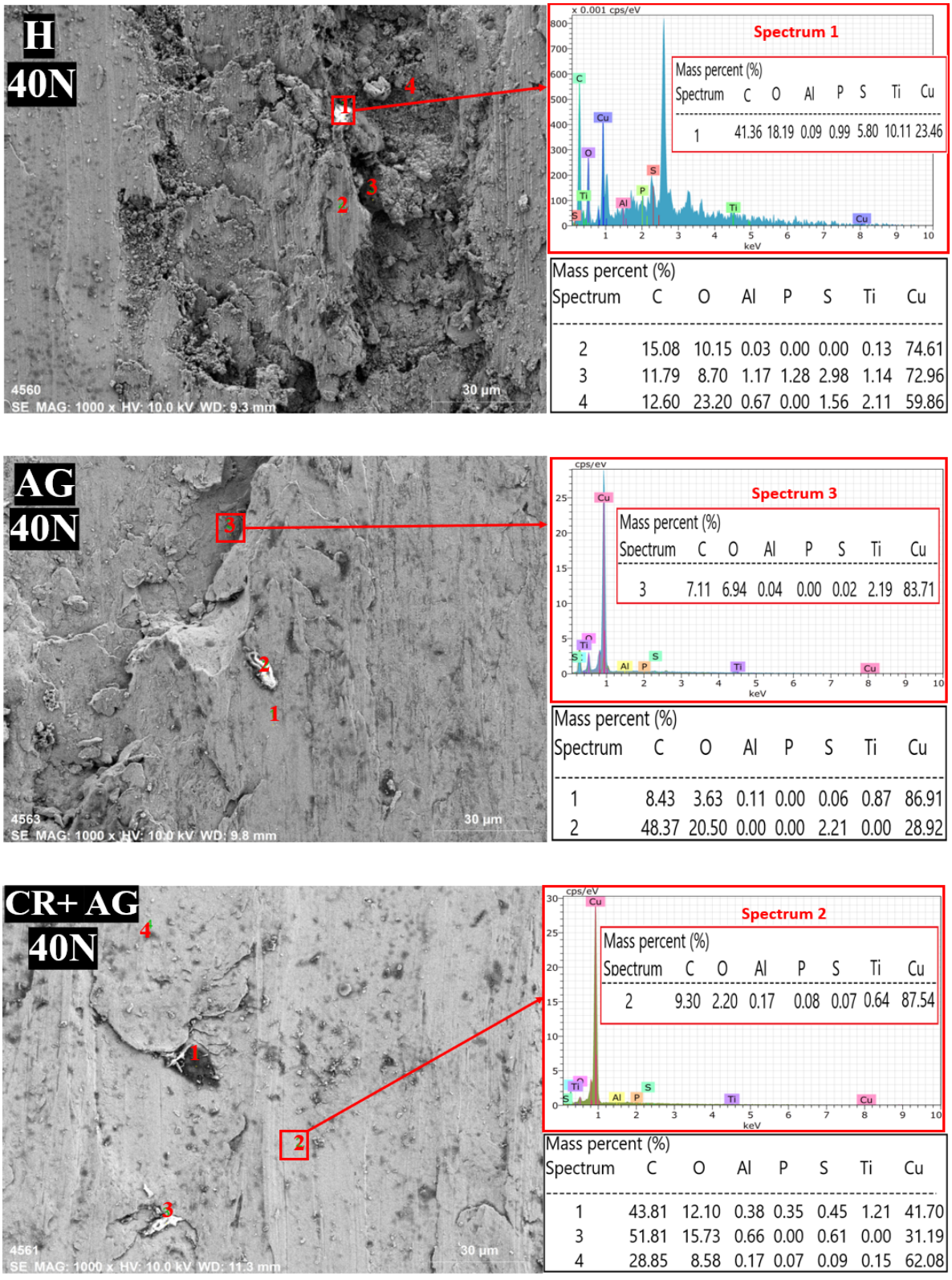

Fig. 14. EDX analysis of worn surfaces of Cu-2.5Ti alloy samples under the load of 40 N under dry environment

ion can accelerate the dissolution of metal and can react with the metal to compose some kind of metal chloride compounds. Generally, seawater corrosion contributes to the specific wear rate of specimens in the seawater environment. However, the corrosion products decreased the contact area of the ball and the specimen during the sliding process, and therefore the corrosion products showed a lubricating effect [22,26]. This is because why the wear rates are decreased in the corrosive environment. To compare the wear test in two environments, it can be seen that the smeared layer is thinner in a corrosive environment than the dry one because of the lubricating effect of corrosion products and water. Also, large flake debris appearances are more

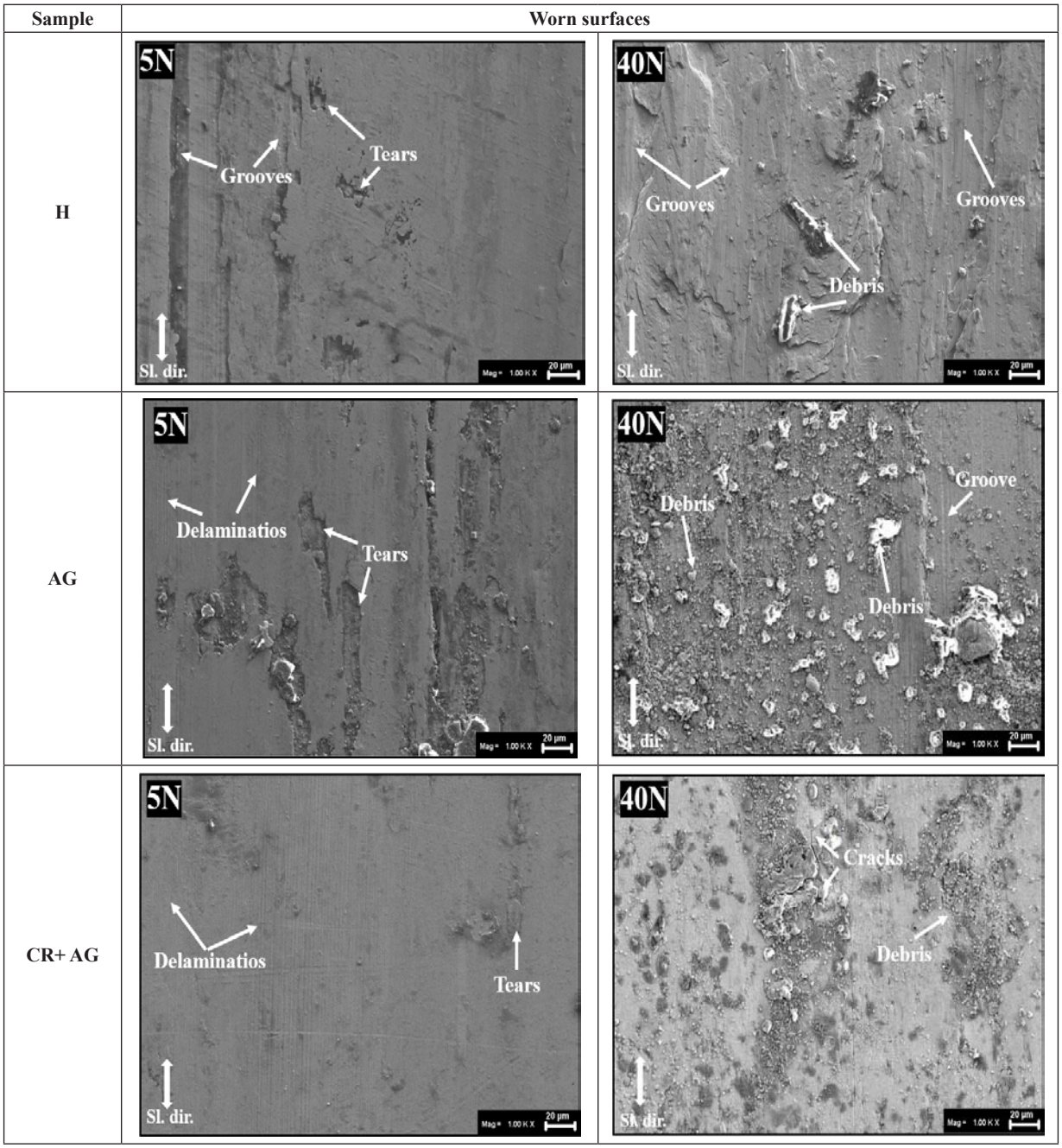

Fig. 15. SEM micrographs showing the worn surfaces of the Cu-2.5Ti alloy samples under a corrosive environment

visible in a dry environment than the corrosive ones. Another point to be noted is the existence of an oxidative wear regime during rubbing for both samples in the corrosive atmosphere from the mass percent of oxygen in the EDX analysis as seen in Fig. 16.

4. Conclusions

Cu-2.5%Ti alloy was studied by using pure electrolytic copper and titanium metal melted under an argon atmosphere in an induction vacuum. Homogenized, aged, and prior cold-rolled and aged samples produced after successful thermal processes. The role of microstructure and its influence on the values of friction coefficient and degree of wear tribological tests were analyzed and the following conclusions are drawn.

- Cu-2.5Ti alloy of H sample contains a single supersaturated Cu solid solution phase with recrystallization grains (polygonal grains). Ti-rich small precipitates can be seen at grain boundaries. The aged sample (AG), fine needle-shaped precipitates dispersed throughout the grain, and a small number of cellular precipitates advancing from the grain boundaries into the grains are seen together. From EDX analysis fine precipitates consisting of coherent, metastable, and continuous β-Cu_3Ti phase with a body-centered tetragonal structure are observed in the AG sample.
- During the initial sliding distance, the frictional coefficient had remained unstable for both samples and then maintained

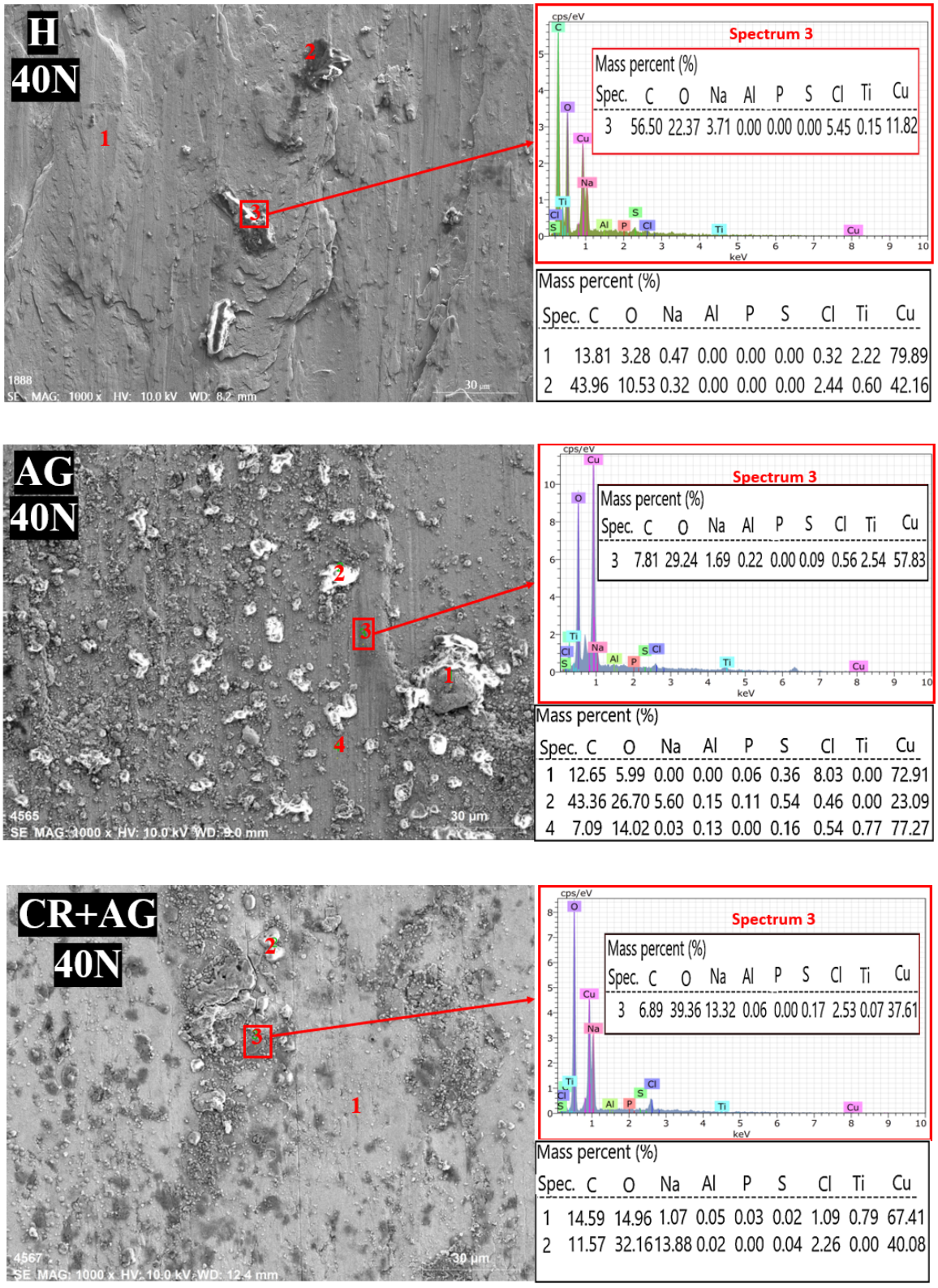

Fig. 16. EDX analysis of worn surfaces of Cu-2.5Ti alloy samples under the load of 40 N under corrosive environment

a nearly steady-state (after ~100 m) until the termination of the tests.

- At the applied load. 40 N a high rate of wear occurs for both environments. The decrease in wear rates of the samples (H), (AG), and (CD+ AG) respectively can be attributed to increasing in hardness.
- Under a dry environment the worn surfaces show plastic deformation regions, grooves, and debris. When the load amount is 40 N, it is seen that the samples produce wear residue and adhesive wear predominates in all samples.
- Under the corrosive environment of 3.5% NaCl water solution for all samples the worn surfaces at applied load

5 N some tears have occurred. The surface morphology is relatively smooth for 5 N and when the load is 40 N, the smoothness of the surface deteriorates due to the increasing amount of load.

- Under the corrosive environment, the chloride ion can accelerate the dissolution of metal and can react with the metal to compose some kind of metal chloride compounds The corrosion products showed a lubricating effect. This is because why the wear rates are decreased in the corrosive environment.

Additional information

The authors disclosed receipt of the following financial support for the research, authorship, and/or publication of this article: The study was supported by Karabuk University Scientific Research Projects Unit (KBU-BAP) with Project No. KBU-BAP- 17- DR- 272

REFERENCES

[1] W.A. Soffa, D.E. Laughlin, P. Mat. Sci. **49**, 347-366.(2004). DOI: https://doi.org/10.1016/S0079-6425(03)00029-X

[2] A. Szkliniarz, L. Blacha, W. Szkliniarz, J. Labaj, Arch. Metall. Mater. **59**, 1307-1312 (2014). DOI: https://doi.org/10.2478/amm-2014-0223

[3] S. Semboshi, S. Amano, J. Fu, A. Iwase, T. Takasugi, Metallurgical and Materials Transactions A **48**, 1501-1511 (2017).

[4] R. Markandeya, S. Nagarjuna, D.S. Sarma, Mater. Sci. Eng. **A 404**, 305-313 (2005). DOI: https://doi:10.1016/j.msea.2005.05.072

[5] S. Kim, M. Kang, J. Ind. and Eng. Chem. **18**, 969-978 (2012). DOI: https:// doi.org/10.1016/j.jiec.2011.10.009

[6] S. Nagarjuna, K. Balusabramanian, D.S. Sarma, Mater. Sci. Eng. **A 225**, 118-124 (1997). DOI: https://doi.org/10.1016/S0921-5093(96)10578-5

[7] R. Markandeya, S. Nagarjuna, D.S. Sarma, Mater. Charac. **57**, 348-357 (2006). DOI: https://doi.org/10.1016/j.matchar.2006.02.017

[8] A. Szkliniarz, Arch. Metall. Mater. **62**, 223-230 (2017). DOI: https://doi.org/10.1515/amm-2017-0033

[9] S. Nagarjuna, K. Balusabramanian, D.S. Sarma, J. Mater. Sci. **34**, 2929-2942 (1999). DOI: https://doi.org/10.1023/A:1004603906359

[10] S. Nagarjuna, M. Srivinas, Mater. Sci. Eng. A **498**, 468-474 (2008). DOI: https://doi.org/10.1016/j.msea.2008.08.029

[11] S. Nagarjuna, K. Balusabramanian, D. Sarma, J. Mater. Sci. **32**, 3375-3385 (1997). DOI: https://doi.org/10.1023/A:1018608430443

[12] S. Suzuki, K. Hirabayshi, H. Shibata, K. Mimura, M. Isshiki, Y. Waseda, Scripta Materialia **48**, 431-435 (2003). DOI: https://doi.org/10.1016/S1359-6462(02)00441-4

[13] S. Semboshi, S. Orimo, H. Suda, W. Gao, A. Sugawara, Mater. Transactions **52**, 2137-2142 (2011). DOI: https://doi.org/10.2320/matertrans.M2011173

[14] T. Hakkarainen. D. Tech thesis Formation of coherent Cu4Ti precipitates in copper-rich copper-titanium alloys: Dissertation, Helsinki University of Technology, Helsinky, Finland (1971).

[15] D. Laughlin, J.V. Cahn, Acta Metallurgica **23**, 329-339 (1975). DOI: https://doi.org/10.1016/0001-6160(75)90125-X

[16] R.C. Ecob, J.V. Bee, B. Ralph, Metallurgical Transactions **A 11**, 1407-1414 (1980). DOI: https://doi.org/10.1007/BF02653496

[17] J. Dutkiewicz, Metallurgical Transactions A **8**, 751-761 (1977). DOI: https://doi.org/10.1007/BF02664785

[18] M.J. Saarivirta, H.S. Cannon, Copper-titanium alloys, Metal. Progress. **76**, 2 81-84 (1959).

[19] S. Nagarjuna, K. Balusabramanian, D.S. Sarma, Mater. Transactions. **36**, 1058-1066 (1995). DOI: https://doi.org/10.2320/matertrans1989.36.1058

[20] Z. Boumerzoug, J. Mater. Eng. Tech. **003**, 57-62 (2020).

[21] M. Sundberg, R. Sundberg, S. Hogmark, R. Otterberg, B. Lehtinen, S. E. Hörnström, S.E. Karlsson, Wear **115**, 151-165 (1987). DOI: https://doi.org/10.1016/0043-1648(87)90206-7

[22] F. Zhou, Y. Wang, H. Ding, M. Wang, M. Yu, Z. Dai, Surface & Coating Tech. **202**, 3808-3814 (2008). DOI: https://doi.org/10.1016/j.surfcoat.2008.01.025

[23] P.S. Blau, Tribology International **34** (9), 585-591 (2001). DOI: https://doi.org/10.1016/S0301-679X(01)00050-0

[24] F. Aydın, Y. Sun, Can, Metall. Quart. **57**, 1-15 (2018). DOI: https://doi.org/10.1080/00084433.2018.1478491

[25] G. Chassaing, L. Faure, S. Philippon, Wear **320**, 25-33 (2014). DOI: https://doi.org/10.1016/j.wear.2014.08.001

[26] J.F. Archard, Journal of Applied Physics **24** (8), 981-988 (1953). DOI: https://doi.org/10.1063/1.1721448